# RSC Advances

**Synthesis of Ag-Ni core-shell nanowires and their application in anisotropic transparent conductive films**

Bo-Tau Liu,[1,*] Shao-Xian Huang,[1] Mei-Feng Lai,[2,3] and Zung-Hang Wei[2]

[1]Department of Chemical and Materials Engineering
National Yunlin University of Science and Technology
Yunlin 64002, Taiwan

[2]Institute of NanoEngineering and MicroSystems
National Tsing Hua University
Hsinchu 30013, Taiwan

[3]Department of Power Mechanical Engineering
National Tsing Hua University
Hsinchu 30013, Taiwan

---

*Corresponding author: Department of Chemical and Materials Engineering, National, Yunlin University of Science and Technology, 123 Univ. Rd., Sec. 3, Douliou, Yunlin 64002, Taiwan, ROC. Tel.: 886-5-534-2601. Fax: 886-5-531-2071.
E-mail address: liubo@yuntech.edu.tw (B.-T. Liu).

**ABSTRACT**

We report a modified two-step method for the synthesis of highly dispersed and

conductive Ag-Ni core-shell nanowires. The conductivity of the nanowire networks

was improved by thermal treatment under various atmospheres. $H_2$-thermal treatment

shows the superior enhancement on electrical conductivity and reduces the sheet

resistance by nearly seven orders of magnitude relative to that of the pristine networks.

X-ray photoelectron spectroscopy analysis reveals that the metallic $Ni^0$ faction on the

surface is more important than Ni amount on the surface to the electrical conductivity.

The transparent conductive films of Ag-Ni nanowires have sheet resistance of 220

$\Omega$/sq at a transmittance of 75%, much better than those made from the pure Ni

nanowires. The Ag-Ni nanowires were aligned easily by applying an external

magnetic field; the anisotropic conductivity ratio for the corresponding transparent

conductive films can be larger than $10^5$. The well performance may be attributed to

the fact that the as-prepared nanowires possess moderate saturation magnetization and

low coercivity, alleviating the aggregation of nanowires and favoring the nanowire

alignment.


Key words: Ag-Ni nanowire; core-shell; anisotropic transparent conductive film;

         magnetic field

1. **Introduction**

Although metals possess excellent electrical conductivity in nature, they can't be used

directly as electrodes in optoelectronic products such as touch sensors, liquid crystal

displays, solar cells, and organic light emitting diodes, owing to the high extinction

coefficient and the opaque characteristic in the visible-light region. In order to own

both transparency and conductivity, indium tin oxide (ITO) is the most commonly

used material in the manufacture of transparent conductive electrodes or films (TCFs).

Recently, some new materials, including carbon nanotubes,[1, 2] graphene nanosheets,[3]

silver-particle grid,[4] and silver nanowires (AgNWs),[5, 6] have been investigated widely

as potential replacements for ITO in TCFs to improve the main drawbacks of ITO:

inflexibility, the limited supply of indium, and poor conductivity for plastic substrates

due to incapable of high-temperature annealing.[7, 8] To increase the transparency of

electrodes, the candidate materials usually appear in the form of nanowires or

nanotubes to create voids allowing light to pass through. Among the potential

candidates, silver materials show the highest ratio of DC conductivity to optical

conductivity ($\sigma_{DC}/\sigma_{OP}$),[9] which is a key figure of merit for transparent conductive

electrodes. Very recently, TCFs of AgNWs have been applied commercially in touch

sensors by TPK Co.

In the AgNW films, the AgNWs are distributed randomly and disorderly. It is

more difficult to assemble the nanowires into orientational structures or ordered

arrays due to the occurrence of curling and twisting among the nanowires with

extra-large aspect ratio. Recently, some studies have reported the aligned AgNWs

could be achieved by Langmuir-Blodgett technique,[10] washing process,[11]

polyvinylpyrrolidone (PVP) interaction,[11-14] various kinds and flow directions of

solvents,[13] oil-water-air interface,[14] and graphene oxide assistant,[15] etc. Although

these methods have been shown pleasing results, they are difficult to be applied in the

practical manufacture process for optoelectronic devices due to the rigorous

preparation conditions and the caprice of solvent evaporation. A reliable method is to

apply an external force such as magnetic field to drive the nanowires into alignment.

Nickel or cobalt is a ferromagnetic material and their nanowires can be aligned by

applying a magnetic field, showing enhancement of mechanical properties[16] and vary

high anisotropic electrical behaviors.[17] However, magnetic materials usually possess

poor electrical conductivity, against application for TCFs. Combining with

high-electrical-conductivity metals such as silver and copper, the hybrid nanowires

are supposed to possess higher electrical conductivity. However, studies that describe

the preparation of the bi-metal nanowires are still few in the literature. Zhang and

Zeng synthesized the Cu-Ni core-shell nanowires with 200-300 nm in diameter by a

one-pot synthesis method and the corresponding magnetic properties were also

analyzed.[18] Rathmell et al. prepared the Cu-Ni core-shell nanowires by a two-step

approach to improve the limitation of the work of Zhang and Zeng (too large diameter

and narrow formula window).[19] The as-prepared Cu-Ni nanowires in transparent

conductive films showed remarkable resistance to oxidation. McKiernan et al.[20]

fabricated the Ag-Ni core-shell nanowires by a two-step approach. The electrical and

magnetic properties of the nanowires were further discussed. However, they found

that the electrical conductivity of the hybrid nanowires was two orders of magnitude

lower than that of bulk Ag or Ni. The hybrid nanowires were also exhibited superior

catalytic activity for the $H_2$ generation from ammonia borane compared to the pure Co

and Ni nanoparticles.[21, 22]

Although the aligned metal nanowires has been reported to possess excellent

surface enhanced Raman spectroscopy effect,[23] mechanic enhancement,[16] and

anisotropic electrical properties,[17] to the best of our knowledge, no study has

investigated high-performance anisotropic TCFs. This may be because the electrical

conductivity of the pure magnetic-metal nanowires is too low or the core-shell

bi-metal nanowires aren't dispersed well and entwine each other. In this study, we

fabricate highly dispersed and conductive Ag-Ni core-shell nanowires by a modified

two-step method. The electrical, magnetic, and surface properties of the nanowires

were further investigated. The anisotropic TCFs were made from the nanowires. The

anisotropic characterization of the TCFs was analyzed and discussed.

## 2. Experimental

2.1 Materials

Silver nitrate ($AgNO_3$, Sigma–Aldrich), nickel nitrate ($Ni(NO_3)_2$, Showa), PVP (MW: 40000, Sigma–Aldrich),, ethylene glycol (EG, Showa), sodium chloride (Katayama Chem.), N,N-diethylhydroxylamine (DEHA), and hydrazine (Showa) were used as received. Reagent-grade solvents and deionized water (DI water, >18 MΩ·cm) were used throughout the experiments.

2.2 Preparation of Ag-Ni core-shell nanowire

The Ag-Ni core-shell nanowires were fabricated using a two-step method, similar to the previous report,[19] with preparation procedure modified to obtain more dispersible and higher-yield nanowires, which is in favor of the production of TCFs. PVP and DEHA were added into the silver nanowire EG solution synthesized as reported in our previous study (see supplementary information),[24, 25] at final concentration of 1 wt%. 46.16 g of 2 wt% PVP, 6.88 g of 0.1 M $Ni(NO_3)_2$, and 32 g of the silver nanowire mixture were mixed and stirred at 600 rpm in a reaction vessel and heated at 120 ℃ by a simple straight-blade PTFE turbine under $N_2$ atmosphere. After 5 min, 5.66 g of 35 wt% hydrazine in water was added slowly using a peristaltic pump. When the

color of the solution turned from silver-whitish to black, the nickel ions were reduced

to metallic nickel on the surface of AgNWs to form the Ag-Ni core-shell structure.

The as-prepared core-shell nanowires were washed three times with ethanol through

centrifugation and then purified using magnetic separation.

2.3 Preparation of anisotropic TCFs and thermal treatment

Glass substrates were washed with ethanol and cleaned using an $O_2$ plasma cleaner

(PDC-23G, Harrick Plasma). The various amounts of the10-mg/mL Ag-Ni NW

solution (listed in Table 2) was dropped and then spin-coated on a treated glass

substrate of 2.5 cm x 2.5 cm (100 rpm, 5 s). Before the solution was dried, the coated

substrate was placed immediately in a magnetic device with 100 mT magnetic flux

density. Until the solvent was evaporated completely, the coated substrate was token

out from the magnetic device for further measurement and investigation. As for the

thermal treatment, the aligned nanowire films were placed in an air, $N_2$ or $H_2$

atmospheres at 200℃ for 20 min.

2.4 Characterization

The morphologies of the nanowires and the TCFs were examined using an optical

microscope (OM, M835, M&T Optics) and a field-emission scanning electron

microscope (SEM; JSM-7401F, JEOL). The core-shell structure was characterized

using a high resolution transmission electron microscope (TEM; JSM 7401F, JEOL)

and an X-ray diffractometer (Miniflex II, Rigaku). The elemental analysis and binding

energy of the surface of the nanowires were determined by X-ray photoelectron

spectroscopy (XPS) (PHI 5000 VersaProbe, ULVAC-PHI) at a take-off angle of $90^0$.

The sheet resistances of the transparent conductive electrodes were determined using

a four-pin probe meter (Loresta-GP, Mitsubishi Chemical) with an MCP-T610 probe.

The transmittance and UV-Vis spectra were measured using an UV–Vis

spectrophotometer (Lambda 850, PerkinElmer). The magnetic hysteresis curve for the

Ag-Ni core-shell nanowires was measured using a superconducting quantum

interference device magnetometer (MPMS5, Quantum Design).

## 3. Results and discussion

In the Ag-Ni core-shell synthesis, if the AgNWs were solved in aqueous solution with

no stirring for the Ni coating reaction as reported elsewhere,[19] the reaction produced a

very small amount of the Ag-Ni core-shell nanowires and the nanowires were easy to

aggregate. Because the AgNWs have better suspension stability in EG than water, the

EG was used as solvent in our experiment. Moreover, we found that the Ni coating

reaction with a non-magnetic stir would make the Ag-Ni core-shell nanowires more

dispersible, less aggregate, and more productive compared to no stirring and magnetic

stirring.[20] The non-magnetic stirring was supposed to make the coating solution more

uniform. The as-prepared Ag-Ni core-shell nanowire solution reveals a stable

dispersion (Fig. 1a) and well magnetic separation (Fig 1b).

The diameter of the pristine AgNWs is over 60-100 nm, with average diameter of ~

90 nm (Fig. 2a). After Ni coating, the diameter of the nanowires and its average

increase to 140-190 and 160 nm, respectively (Fig. 2b). The surface of as-prepared

Ag-Ni nanowires reveals rough and is mainly composed of nickel (Fig. 2c).

According to these results, the Ag-Ni nanowires are supposed as core-shell structure

and the thickness of the Ni shell can be estimated approximately to 35 nm. Fig. S1

displays the XRD patterns of AgNWs and Ag-Ni nanowires. Although the

characteristic peaks of Ni corresponding to (111) and (220) planes overlap with those

of Ag with respect to (111) and (311) planes, the peak at $51.7^{o}$ corresponds to (200)

plane, suggesting that the Ni shell is polycrystalline with a grain size of 11.4 nm

calculated from the peak of (200) plane using Sherrer's equation. The surface plasmon

resonance peaks of AgNWs appearing at 350 and 386 nm, corresponding respectively

to the out-of-plane quadrupole resonance and the out-of-plane dipole resonance

modes,[26, 27] are suppressed and broadened while the Ni shell is coated over the surface

of AgNWs (Fig. S2). The observation is in good agreement with the finding in Ag-Ni

core-shell nanoparticles.[28]

The as-prepared Ag-Ni nanowires possess poor electrical conductivity.

According to the AgNW experiences, the conductivity is often able to be improved by the post-thermal treatment due to the decomposition and/or flowing of dispersants attaching to the surface of nanowires, allowing nanowires to contact tightly and fuse together and therefore reducing the junction resistance among nanowires.[29] Therefore, to increase the conductivity, the Ag-Ni core-shell networks were treated thermally under various atmospheres. Fig. 3 shows the improvement on electrical conductivity by the thermal treatment; the sheet resistance reduces in the following sequence: pristine > air > $N_2$ > $H_2$. $H_2$-thermal treatment shows the superior enhancement on electrical conductivity compared to air and $N_2$ atmospheres and reduces the sheet resistance by nearly seven orders of magnitude relative to that of the pristine TCFs. To realize the cause of the enhancement, we carried out the photoelectron spectroscopic chemical analysis on the surface of Ag-Ni nanowires. Fig. 4a reveals two primary peaks in the $O_{1s}$ spectrum: one at near 528.8 eV is attributed to NO; the other at 530.8 eV corresponds to hydroxide species or $Ni(OH)_2$.[30, 31] The intensity ratio of $Ni(OH)_2$ to NO follows the order: pristine > air > $N_2$ > $H_2$, which is the same order as the reduction of sheet resistance. Fig. 4b displays two peaks at 851.8 and 855 eV in the $Ni2p_{3/2}$ spectrum for metallic $Ni^0$ and ionic-state $Ni^{2+}$, respectively.[32, 33] $N_2$- and $H_2$-thermal treatments (especially $H_2$) increase the metallic $Ni^0$ remarkably, whereas the increase is not observed for air-thermal treatment. Table 1 shows the C, O, and Ni

fractions as well as their ratios on the surface of Ag-Ni nanowires. Air-thermal

treatment increases the oxygen fraction on the surface, whereas $H_2$-thermal treatment

shows the largest Ni-atom recovery. All of the thermal treatments reduce the ratios of

C/Ni and O/Ni. Based on the aforementioned results, we conclude that thermal

treatment may lead to the removal of hydroxyl groups or adsorbed water and the

decomposition of PVP on the nanowire surface and consequently reduce the junction

resistance among nanowires; $N_2$- and $H_2$-thermal treatments show better ability on

reduction of $Ni^{2+}$ to $Ni^0$ than air one. Comparing Figs. 3, 4 and Table 1, the valance of

Ni on the surface is more important than the kinds of functional groups or Ni amount

on the surface to the electrical conductivity; the metallic $Ni^0$ faction on the surface

plays a key role on the sheet resistance of TCFs of Ag-Ni core-shell nanowires. The

re-oxidation is unobservable over 2 weeks after thermal annealing at room

temperature. To increase the reliability, incorporating polyethoxysiloxane into the

nanowire layer has been suggested to enhance the resistance to oxidation and thermal

shock.[25]

Fig. 5 presents the variation of the sheet resistance of the TCFs of Ag-Ni

nanowires after thermal treatment transmittance at an incident light of 550 nm. At a

transmittance of 75%, the sheet resistance of the TCFs is near 220 $\Omega$/sq. The

performance is worse than that of the pure AgNWs.[25] Roughly speaking, the Ni

coating reduces the electrical conductivity by nearly 1 order of magnitude relative to

that of the AgNW networks. However, our work revealed superior electrical

conductivity for the Ag-Ni NWs compared to the result reported in the literature.[20] We

infer that the enhancement may arise from the different preparation/measurement

methods and the post-thermal treatment. Nevertheless, the electrical conductivity of

the Ag-Ni NWs is much better than that of the pure Ni nanowires.[17]

The as-prepared Ag-Ni nanowires can be aligned easily in an applied magnetic

field and show anisotropic characteristics (Fig. 6). In order to analyze the anisotropic

properties, we prepared the Ag-Ni networks by a quantitative spinning method.[24] As

can be seen in Table 2, the anisotropic conductivity ratio ($R_\perp/R_{II}$) can be larger than

$10^5$ due to the alignment of nanowires. However, the anisotropic conductivity ratio

decreases with the increase of the nanowire amount. It is easy to figure out that the

increase of nanowire amount will increase the probability that they touch side by side

and thereby increase the conductivity in the transverse direction, resulting in the

decrease of the anisotropic conductivity ratio. Nevertheless, the TCFs still have the

anisotropic conductivity ratio of 1.5 when the sheet resistance of the TCFs reaches 23

$\Omega$/sq. Fig. 7 presents the magnetization curve of Ag-Ni nanowires. The saturation

magnetization of the as-prepared Ag-Ni core-shell nanowires is 22.94 emu/g, based

on the total mass of Ag and Ni. When only the mass of Ni is considered, the saturation

12

magnetization is calculated to the value of 35.5 emu/g (using the Ag core of 90 nm

and the Ni shell thickness of 35 nm), which is lower than that of bulk Ni but close to

that of the Ni nanoparticles (34.73 emu/g).[22] However, the coercivity of our Ag-Ni

nanowires is 61 Oe, which is lower than what was reported for Ag-Ni (116 Oe) [20] or

Cu-Ni (237.2 Oe) [18] core-shell nanowires in the literature. Moreover, Remanence of

our samples (3.85 emu/g) is also lower than that reported for Cu-Ni (15.7 emu/g)[18].

The reason for the lower coercivity is not cleat at present, but it may result from the

fact that the Ni grain size for our samples (11.4 nm) is smaller than the Ni critical

diameter (55 nm).[34] The moderate saturation magnetization can avoid that Ag-Ni

nanowires concentrate at the two ends of the applied magnetic field; the low

coercivity and remanence can alleviate the aggregation of nanowires due to the

induced magnetic force after the applied magnetic field is removed. Therefore, the

as-prepared Ag-Ni nanowires are suitable for the preparation of anisotropic TCFs

using an applied magnetic field. Although the resistance to oxidation

## 4. Conclusion

We have fabricated highly dispersed and conductive Ag-Ni core-shell nanowires by a

modified two-step method. The nanowires with moderate saturation magnetization

and low coercivity/remanence reveal a stable dispersion and well magnetic separation.

The TCFs made from the nanowires show the better conductivity and transmittance than that made from the pure Ni nanowires; the sheet resistance of the TCFs can reduce as low as 220 $\Omega$/sq at a transmittance of 75%. We found that the metallic $Ni^0$ faction on the surface is more important than Ni amount on the surface to the electrical conductivity and plays a key role on the sheet resistance of TCFs of Ag-Ni core-shell nanowires. The anisotropic conductivity ratio of the anisotropic TCFs can be larger than $10^5$. Although the ratio decreases with the increase of the nanowire amount, the TCFs still have the anisotropic conductivity ratio of 1.5 even when the sheet resistance of the TCFs reaches 23 $\Omega$/sq.

**Acknowledgments**

14

**References**

1.    Z. Wu, *Science*, 2004, **305**, 1273-1276.

2.    B. T. Liu, C. H. Hsu and W. H. Wang, *J. Taiwan Inst. Chem. Eng.*, 2012, **43**,
      147-152.

3.    L. G. De Arco, Y. Zhang, C. W. Schlenker, K. Ryu, M. E. Thompson and C. W.
      Zhou, *ACS Nano*, 2010, **4**, 2865-2873.

4.    B. Y. Ahn, D. J. Lorang and J. A. Lewis, *Nanoscale*, 2011, **3**, 2700-2702.

5.    A. R. Madaria, A. Kumar, F. N. Ishikawa and C. W. Zhou, *Nano Research*, 2010,
      **3**, 564-573.

6.    C. H. Liu and X. Yu, *Nanascale Res. Lett.*, 2011, **6**, 75.

7.    A. Rahy, P. Bajaj, I. H. Musselman, S. H. Hong, Y.-P. Sun and D. J. Yang, *Appl.
      Surf. Sci.*, 2009, **255**, 7084-7089.

8.    B. T. Liu and C. H. Hsu, *J. Colloid Interface Sci.*, 2011, **359**, 423-427.

9.    X. Y. Zeng, Q. K. Zhang, R. M. Yu and C. Z. Lu, *Adv. Mater.*, 2010, **22**,
      4484-4488.

10.   D. Whang, S. Jin, Y. Wu and C. M. Lieber, *Nano Lett.*, 2003, **3**, 1255-1259.

11.   Y. P. Bi, H. Y. Hu and G. X. Lu, *Chem. Commun.*, 2010, **46**, 598-600.

12.   Y. Gao, P. Jiang, D. F. Liu, H. J. Yuan, X. Q. Yan, Z. P. Zhou, J. X. Wang, L.
      Song, L. F. Liu, W. Y. Zhou, G. Wang, C. Y. Wang and S. S. Xie, *Chem. Phys.
      Lett.*, 2003, **380**, 146-149.

13.   P. Jiang, S. Y. Li, S. S. Xie, Y. Gao and L. Song, *Chem Eur. J.*, 2004, **10**,
      4817-4821.

14.   H. Y. Shi, B. Hu, X. C. Yu, R. L. Zhao, X. F. Ren, S. L. Liu, J. W. Liu, M. Feng,
      A. W. Xu and S. H. Yu, *Adv. Funct. Mater.*, 2010, **20**, 958-964.

15.   Y. G. Li and Y. Y. Wu, *J. Am. Chem. Soc.*, 2009, **131**, 5851-5857.

16. K. Keshoju and L. Sun, *J. Appl. Phys.*, 2009, **105**, 023515.

17. T. Nagai, N. Aoki, Y. Ochiai and K. Hoshino, *ACS Applied Materials & Interfaces*, 2011, **3**, 2341-2348.

18. S. M. Zhang and H. C. Zeng, *Chem. Mater.*, 2010, **22**, 1282-1284.

19. A. R. Rathmell, M. Nguyen, M. F. Chi and B. J. Wiley, *Nano Lett.*, 2012, **12**, 3193-3199.

20. M. McKiernan, J. Zeng, S. Ferdous, S. Verhaverbeke, K. S. Leschkies, R. Gouk, C. Lazik, M. Jin, A. L. Briseno and Y. N. Xia, *Small*, 2010, **6**, 1927-1934.

21. B. L. Sun, M. Wen, Q. S. Wu and J. Peng, *Adv. Funct. Mater.*, 2012, **22**, 2860-2866.

22. M. Wen, B. L. Sun, B. Zhou, Q. S. Wu and J. Peng, *J. Mater. Chem.*, 2012, **22**, 11988-11993.

23. A. Tao, F. Kim, C. Hess, J. Goldberger, R. R. He, Y. G. Sun, Y. N. Xia and P. D. Yang, *Nano Lett.*, 2003, **3**, 1229-1233.

24. B.-T. Liu and H.-L. Kuo, *Carbon*, 2013, **63**, 390-396.

25. B.-T. Liu and S.-X. Huang, *RSC Adv.*, 2014, **4**, 59226-59232.

26. X. L. Tang, M. Tsuji, M. Nishio and P. Jiang, *Bull. Chem. Soc. Jpn.*, 2009, **82**, 1304-1312.

27. Y. Gao, P. Jiang, L. Song, L. Liu, X. Yan, Z. Zhou, D. Liu, J. Wang, H. Yuan, Z. Zhang, X. Zhao, X. Dou, W. Zhou, G. Wang and S. Xie, *J. Phys. D: Appl. Phys.*, 2005, **38**, 1061.

28. M. Tsuji, S. Hikino, M. Matsunaga, Y. Sano, T. Hashizume and H. Kawazumi, *Mater. Lett.*, 2010, **64**, 1793-1797.

29. J. Y. Lee, S. T. Connor, Y. Cui and P. Peumans, *Nano Lett.*, 2008, **8**, 689-692.

30. A. F. Carley, S. Rassias and M. W. Roberts, *Surf. Sci.*, 1983, **135**, 35-51.

31.  M. C. Biesinger, B. P. Payne, L. W. M. Lau, A. Gerson and R. S. C. Smart, *Surf. Interface Anal.*, 2009, **41**, 324-332.

32.  M. Alsabet, M. Grden and G. Jerkiewicz, *Electrocatalysis*, 2014, **5**, 136-147.

33.  J. L. Rodriguez, M. A. Valenzuela, H. Tiznado, T. Poznyak and E. Flores, *J. Mol. Catal. A: Chem.*, 2014, **392**, 39-49.

34.  A.-H. Lu, E. L. Salabas and F. Schüth, *Angew. Chem. Int. Ed.*, 2007, **46**, 1222-1244.

**List of figures**

Table 1. XPS analysis data for the surface of Ag-Ni core-shell nanowires.

| Annealing atmosphere | Composition, at.% | | | Atomic ratio, at./at. | |
|---|---|---|---|---|---|
| | $C_{1s}$ | $O_{1s}$ | $Ni_{2p}$ | $C_{1s}/Ni_{2p}$ | $O_{1s}/Ni_{2p}$ |
| No thermal treatment | 42.70 | 38.69 | 18.61 | 2.29 | 2.08 |
| Air | 32.49 | 41.75 | 25.76 | 1.26 | 1.62 |
| $N_2$ | 39.60 | 38.52 | 21.88 | 1.81 | 1.76 |
| $H_2$ | 33.20 | 36.26 | 30.54 | 1.09 | 1.12 |

Table 2. Anisotropic sheet resistance of the TCFs of Ag-Ni core-shell nanowires.

| Amount | $R_{//}{}^a$, $\Omega/\text{sq}$ | $R_{\perp}{}^b$, $\Omega/\text{sq}$ | $R_{\perp}/R_{//}$ |
|---|---|---|---|
| 50 $\mu$L | 1132 | $> 10^8$ | $> 10^5$ |
| 80 $\mu$L | 73 | 246 | 3.4 |
| 100 $\mu$L | 23 | 34 | 1.5 |

[a] Sheet resistance measured in the magnetic-field direction.

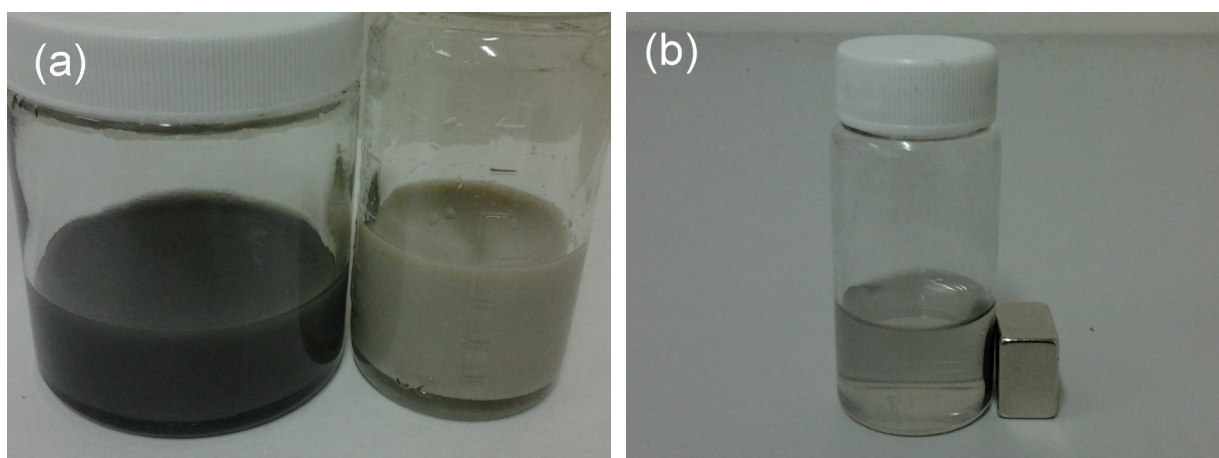[b] Sheet resistance measured in the direction perpendicular to magnetic field.

Fig. 1. Photo images of (a) AgNW solution (right) and Ag-Ni core-shell nanowire solution (left)

and (b) magnetic separation for Ag-Ni core-shell nanowires.
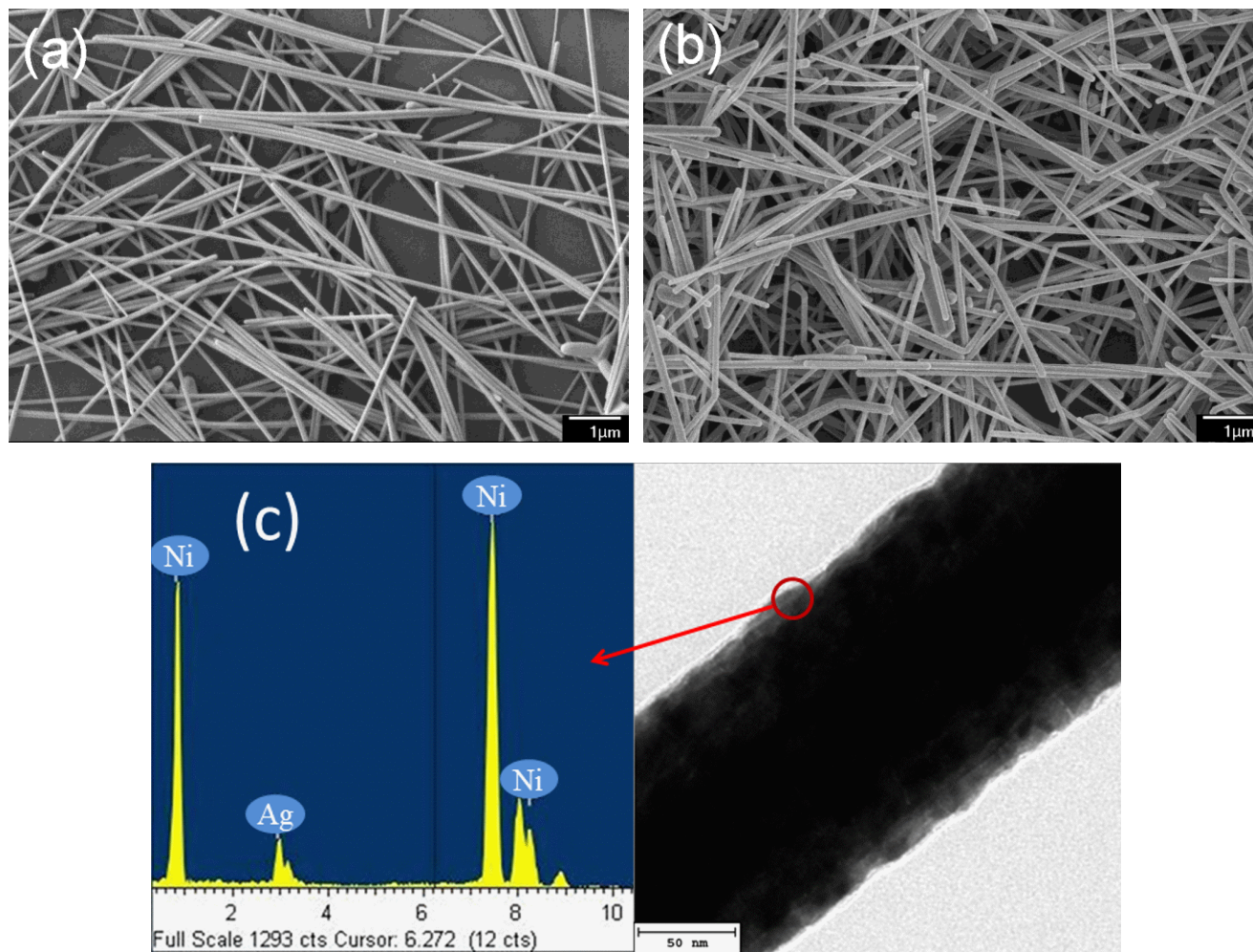
Fig.2. SEM images of (a) AgNWs and (b) Ag-Ni core-shell nanowires and (c) TEM image of a

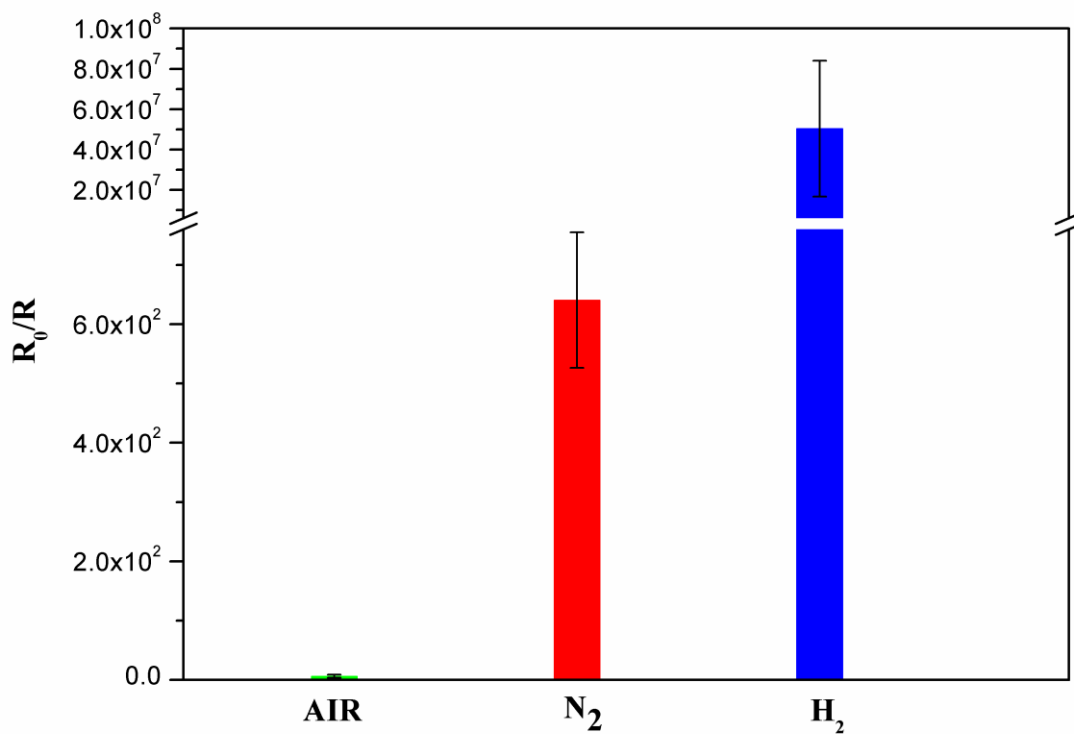Ag-Ni core-shell nanowire with EDS spectra recorded from its surface (indicated region).

Fig.3. Relative sheet resistance of the TCFs of Ag-Ni core-shell nanowires treated thermally under

various atmospheres. $R_0$ is the initial sheet resistance, and R is the sheet resistance after the
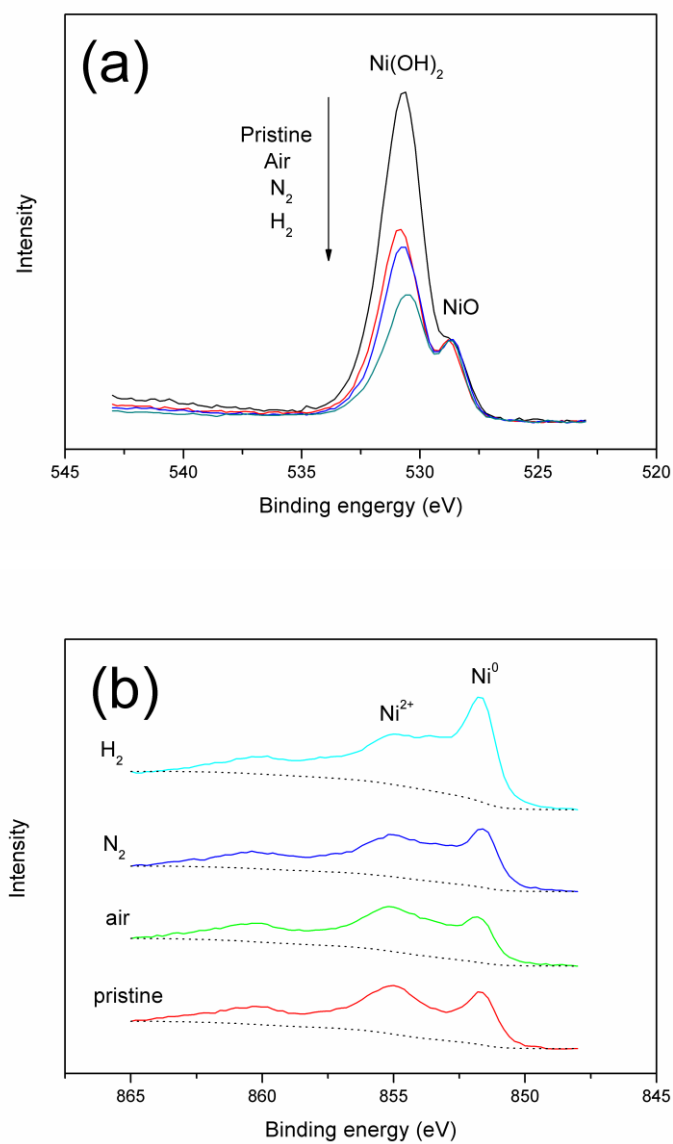
thermal treatment.

Fig.4. XPS spectra of (a) O1s and (b) Ni2p$_{3/2}$ for Ag-Ni core-shell nanowires under various
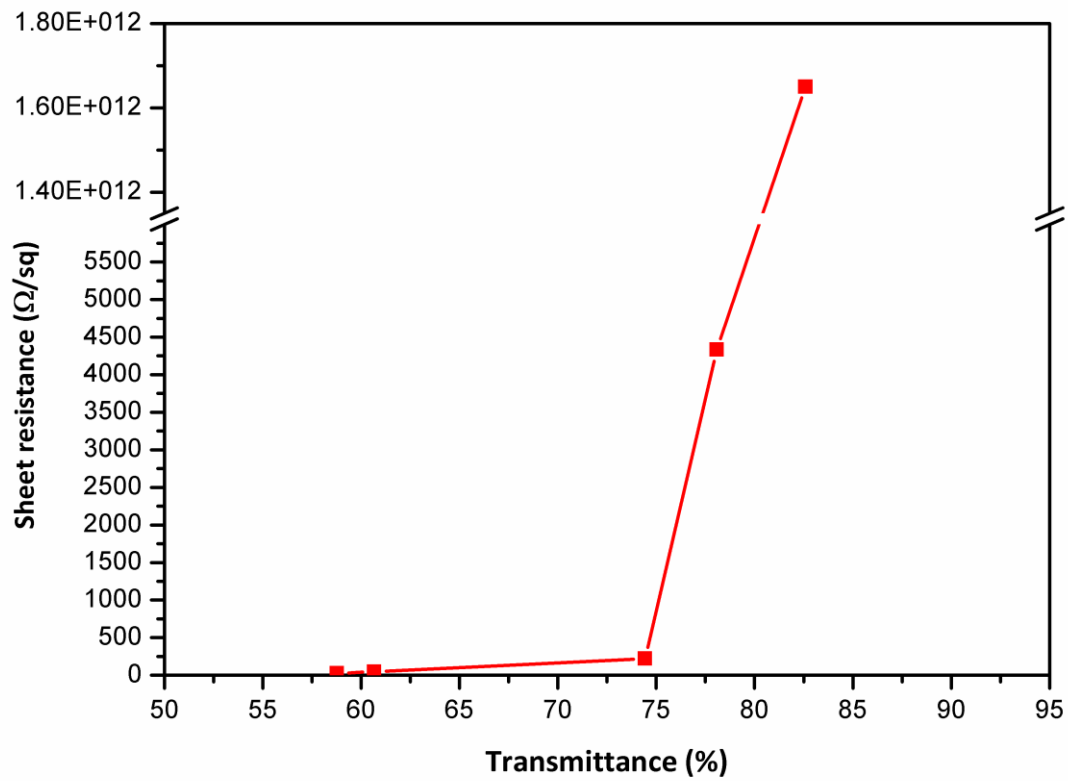
thermal treatments.

Fig.5. Variation of the sheet resistance of the TCFs of Ag-Ni nanowires after $H_2$-thermal treatment

as a function of transmittance at 550 nm.

Fig.6. Photograph of the Ag-Ni nanowire alignment through an applied magnetic field.
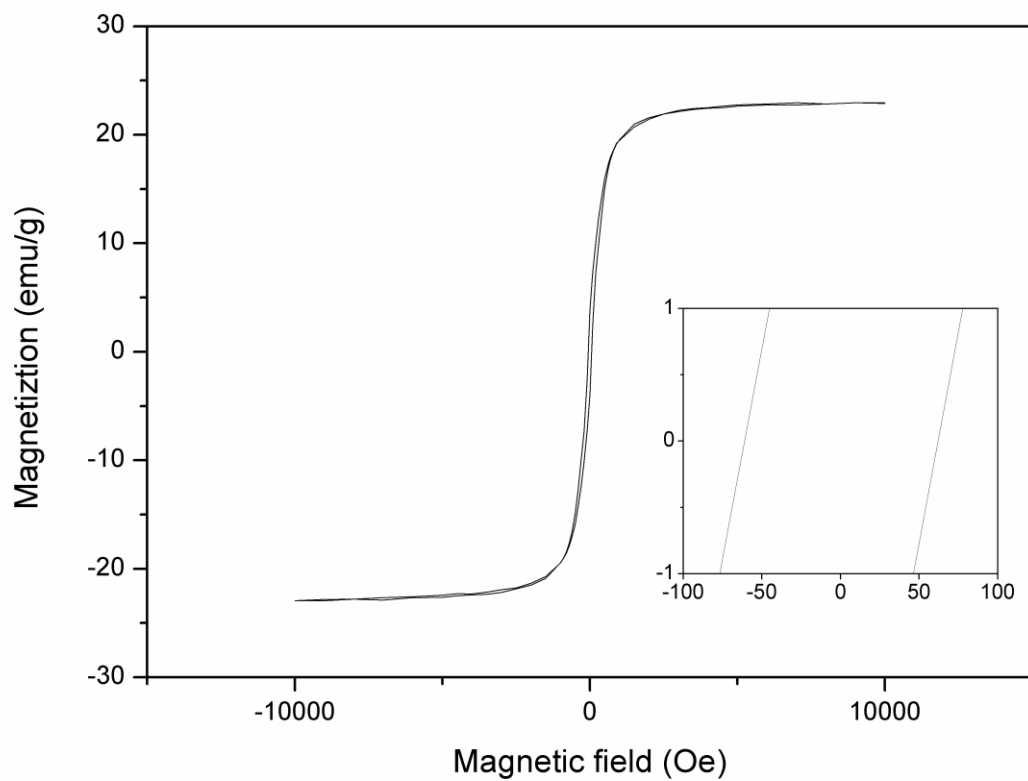
Fig.7. Magnetic hysteresis loop for Ag-Ni core-shell nanowires measured at 300 K. The inset is the

center of the loop.